Implementation of Image Segmentation Techniques to Detect MRI Glioma Tumour

Mid-Level Image-Processing

Siti Rafidah Binti Kassim[1], Setyawan Widyarto[1,2*], Mohammad Syafrullah[2] , Krisna Adiyarta[2], Widya Kumala Sari[3]
[1]Department of Computing, Faculty of Communication, Visual Art and Computing, Kuala Selangor, Malaysia
[2] Program Studi Magister Ilmu Komputer, Universitas Budi Luhur, Jakarta, Indonesia
[3]Alumni of Faculty of Medicine, Universitas Gadjah Mada, Yogyakarta, Indonesia
*Corresponding author: swidyarto@unisel.edu.my

Abstract— **Image identification to detect a tumour needs several stages of image processing along with identifying analysis. To get an accurate segmentation of the tumour contour and to identify brain tumour based on brain magnetic resonance imaging (MRI), a suitable techniques and stages of image processing are required to be applied. One technique of mid-level image processing became an objective this work. The objective of the study is to segment the boundary of tumour by applying the Modification of Region Fitting (MRF) method in term of data fitting. The performance of the Region Scalable Fitting (RSF) method and Modified Region Scalable Fitting (MRSF) is evaluated by comparing the number of iterations. As the result, the MRF method has successfully segmented the initial region of brain tumour images.**

Keywords—segmentation; Modification of Region Fitting (MRF); brain tumour; contour

I. INTRODUCTION

An accurate medical segmentation of brain tumour still somehow faces difficulties in its implementation. Due to difficulties arise from noise, low image contrast, intensity homogeneity and also missing, non-clear edges of tissue in the images, some processing of the images prior to the tumour identification will lead to an accurate result. Furthermore, an image segmentation process could be a kind of mid-level digital image processing following any low-level digital image processing as the segmentation will come out with more meaningful images, thus, easier to analyse. Therefore, the segmentation of brain tumour image became a motivation of the topics.

This paper is intended to discuss implementation of image segmentation techniques, one of the image processing techniques, to detect MRI glioma tumour, one of brain tumour. In this study, the difficulties arise from noise, low image contrast and intensity homogeneity is being considered to make.

Glioma is a common malignant tumour affecting the brain and/or the spine. To detect brain tumour, the brain regions are scanned by computer tomography and magnetic resonance imaging (MRI) techniques. Segmentation techniques are used to obtain information on the boundaries of the different tissues. A low level image processing as pre-processing brain images prior to segmentation implementation of this serial research has been published, the pre-processing used 2D-Sigmoid technique [1]

This paper will discuss a continuation of low to mid-level image processing. This level will result images that can be analysed for tumour detection, border contour between tumour and normal brain cell. The method implemented segmentation techniques to detect MRI glioma tumour five cases.

An accurate and repeatable in order to be clinically useful must be the criteria of the segmentation process. Radiologists have to know an exact region or boundary of tumour in order to get the exact size and shape of the tumour for surgery process. Conducting image segmentation on MRI brain image will increase the accuracy of radiologist's result. The accuracy of the size and shape of the tumour includes the width and height of the tumour growth. Ultimately, the radiologists can identify the types of tumour that appeared in MRI image whether it is malignant or benign.

MRSF method improved the robustness to initialization of RSF method by modified the data fitting term in local fitting energy. The performance of the Region Scalable Fitting (RSF) method and Modified Region Scalable Fitting (MRSF) will be evaluated by comparing the number of iterations. Experimental results show desirable of MRF method in terms of computation efficiency.

II. SEGMENTATION TECHNIQUE

A. Segmentation

The analysis of cancer tissues with image segmentation based on K-means clustering was success to distinguish different tissue types (within 17 tumour or necrotic areas) and their spatial distribution matched consistently with the 18 grayscale images [2]. Thus grayscale images ware used in the project presented in this paper. Moreover, it is reported the technique of segmentation does not address potential errors [3].

B. *Various Techniques in Brain Tumour Detection*

An approach for brain tumour image classification based on transfer learning and fine tuning has been used and the approach of may be used to develop classification system for other body organ MRI images and other medical imaging domain such as such as X-rays, PET and CT [4]. The other approaches, classification and segmentation by utilising deep learning have demonstrated success in mammographic tumour classification, interstitial lung disease classification, brain cancer classification, skin cancer classification, and retinopathy image segmentation [5]. A kind of deep learning by using five MRI images is presented in this paper.

A classification algorithm of adaptive neuro-fuzzy inference system (ANFIS) is another technique for training and classifications phase. Since ANFIS also uses the Artificial Neural Network (ANN) ability to classify data and identify patterns, the ANFIS models have more advantage than Artificial Neural Network (ANN) classification algorithm in having both numerical and linguistic knowledge [6].

III. METHODOLOGY

A. *Implementation of Image Segmentation Techniques*

The proposed of segmentation technique was used in this study is Modification of Region Scalable Fitting (MRF) method.

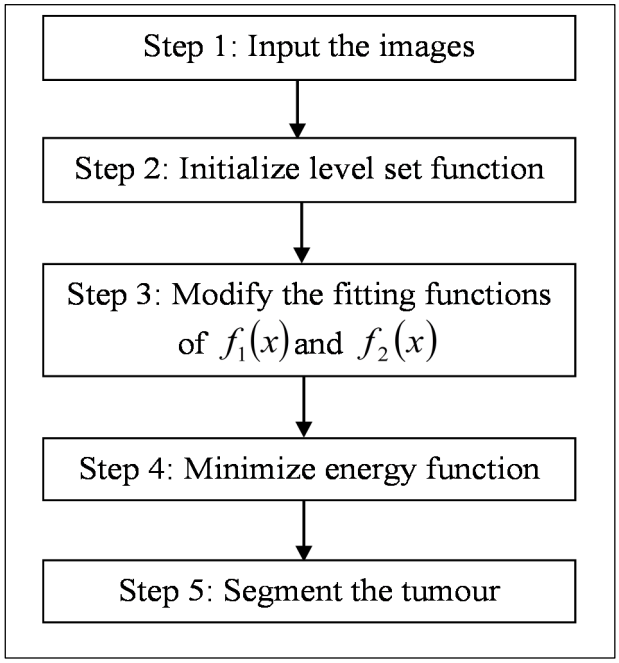

Fig. 1. Flowchart of Modified Region Fitting (MRF).

Step 1: Input the images

Consider a given vector valued image $I : \Omega \rightarrow \Re^n$ where $\Omega \subset \Re^n$ is the image domain and $d \geq 1$ is the dimension of the vector $I(y)$. In particular, d=1 for grey level images.

Step 2: Initialize level set function

Let C be a closed contour in the image domain Ω which separates the Ω into two regions: $\Omega_1 = outside\ (C)$ and $\Omega_2 = inside\ (C)$. For a given point Ω_i the study use the local intensity fitting energy [7] defined as Equation 1.

$$E_x^{Fit}(C, f_1(x), f_2(x)) = \sum_{i=1}^{2} \lambda_i \int_{\Omega_i} K_\sigma(x-y)|I(y)-f_i(x)|^2 dy \quad \text{for} \quad i=1, 2 \tag{1}$$

Where

$E_x^{Fit}(C, f_1(x), f_2(x))$: local intensity fitting energy

C :contour of tumour

λ_i : positive constants for i =1 and 2

$f_1(x)$: approximated the image intensities in Ω_1

$f_2(x)$: approximated the image intensities in Ω_2 .

$K_\sigma(x-y)$: localization of Gaussian kernel.

The localization of Gaussian kernel defined as

$$K_\sigma(x-y) = \frac{1}{\left(\sqrt{2\pi}\sigma\right)^N} e^{-\frac{|x-y|^2}{2\sigma^2}} \tag{2}$$

with scale parameter can only take positive values $\sigma > 0$. The parameter σ determines the width of Gaussian kernel. The term in the Gaussian kernel, $\sqrt{2\pi}\sigma$ is the normalization constant. With the normalization constant this kernel is a normalized kernel. The normalization ensures that the grey level of the image remains the same when blur the image with the kernel.

The intensities $I(y)$ that effectively enrolled in Equation (1) are in a local region centred at the point x, whose size can be controlled by Gaussian kernel. Therefore, Equation (1) defined as modification region fitting (MRF) energy of a contour C at a point x. Whereas, the fitting values approximate the image intensities in a region centred at the point x, whose size can be controlled by the scale parameter σ and 2D sigmoid function in Equation (3).

$$f(x,y) = \frac{1}{1+e^{-\left(\left(\frac{I(x,y)-\beta}{\alpha}\right)\right)}} \tag{3}$$

Where

$f(x,y)$: enhanced pixel value.

$I(x,y)$: intensity of the image at the point (x,y).

α : width of the gradient magnitude around brain image.

B : gradient magnitude around brain image.

The Equation (1), given a centre point *x,* can be minimized when the contour *C* is exactly on the object boundary and the fitting values $f_1(x)$ and $f_2(x)$ optimally approximate the local image intensities on the two sides of *C*. The study finds the contour of *C* that minimizes the energy for all *x* in the image domain, Ω_i, could obtain the entire of object boundary. The process can be achieved by minimizing the integral of Equation (1) over all the centre points in the image domain,Ω. Additionally, to smooth the contour *C* by regularizing its length $|C|$ is necessary in most of the active contours models.

The energy functional of a contour *C* is defined as

$$E(C, f_1(x), f_2(x)) = \int E_x^{Fit}(C, f_1(x), f_2(x))dx + \upsilon|C| \quad (4)$$

Substituting Equation (1) into Equation (4) yields

$$E(C, f_1(x), f_2(x)) = \sum_{i=1}^{2}\lambda_i \int \left[\int_{\Omega_i} K_\sigma(x-y)\,|I(y)-f_i(x)|^2 dy \right] dx + \upsilon|C|$$

for i =1, 2 (5)

where Equation (5) is converted to level set formulation.

Referring to[8] , the level set methods; contour $C \subset \Omega$ is characterized by the zero level set of Lipschitz function $\phi : \Omega \to \Re$ which is called a level set function (LSF). In this study, LSF ϕ is set to be positive and negative values outside and inside the contour *C* respectively [9]. LSF can be simply initialized as a binary step function, which takes a negative constant value -c_0 inside the region R_0 and a positive constant value c_0 outside. Similar to the level set formulation of the RSF, the local intensity fitting energy in Equation (1) can be reformulated in terms of ϕ as follows

$$E_x^{Fit}(\phi, f_1(x), f_2(x)) = \lambda_1 \int_\Omega K_\sigma(x-y)|I(y)-f_1(x)|^2 H(\phi)dy + \lambda_2 \int_\Omega K_\sigma(x-y)|I(y)-f_2(x)|^2 (1-H(\phi))dy \quad (6)$$

where

$H(\phi)$: interior of *C* where *H* is Heaviside function.

$1-H(\phi)$: exterior of *C*

Substitute the Equation (6) into Equation (5), local intensity fitting energy can be rewritten as

$$E(\phi, f_1, f_2) = \lambda_1 \int \left[\int K_\sigma(x-y)|I(y)-f_1(x)|^2 H(\phi)dy \right] dx + \lambda_2 \int \left[\int K_\sigma(x-y)|I(y)-f_2(x)|^2 (1-H(\phi))dy \right] dx + \upsilon \int |\nabla H(\phi)|\, dx \quad (7)$$

The last term $\int |\nabla H(\phi)|\, dx$ in Equation (7) computes the length of the zero level contours. The term is commonly used in variation level set methods for the regularization of the zero level contours [9]. The term $\int |\nabla H(\phi)|\, dx$ can be equivalently expressed as the integral $\int \delta(\phi)|\nabla\phi|\, dx$ with the Dirac delta function, δ. In practice, the Dirac delta function δ and Heaviside function *H* are approximated by the following smooth function δ_ε and H_ε as in many level set methods [9], defined by

$$H_\varepsilon(x) = \frac{1}{2}\left[1 + \frac{2}{\pi}\arctan\left(\frac{x}{\varepsilon}\right)\right] \quad (8)$$

and

$$\delta_\varepsilon(x) = H'_\varepsilon(x) = \frac{1}{2\pi}\left[\frac{\varepsilon}{\varepsilon^2 + x^2}\right] \quad (9)$$

where smoothed Dirac delta function, δ_ε is the first derivative of H_ε with respect to *x*. The parameter of ε is usually set to 1.0 or 1.5. By replacing *H* in Equation (8) with H_ε in the Equation (9), then energy functional in Equation (8) is approximated by

$$E_\varepsilon(\phi, f_1, f_2) = \lambda_1 \int \left[\int K_\sigma(x-y)|I(y)-f_1(x)|^2 H_\varepsilon(\phi)dy \right] dx + \lambda_2 \int \left[\int K_\sigma(x-y)|I(y)-f_2(x)|^2 (1-H_\varepsilon(\phi))dy \right] dx + \upsilon \int |\nabla H_\varepsilon(\phi)|\, dx \quad (10)$$

where $E_\varepsilon(\phi, f_1, f_2)$ is an external energy.

As proposed by [9],

$$P(\phi) = \frac{1}{2}\int (|\nabla\phi| - 1)^2 dx \quad (11)$$

level set regularization term in Equation (11) is added into Equation (7) for penalizes the deviation of the function ϕ from signed distance function (SDF) which can be characterized by the following energy functional.

Add Equation (10) and Equation (11), the entire energy functional in level set formulation is defined as

$$\begin{aligned} MRF(\phi, f_1, f_2) &= E_\varepsilon(\phi, f_1, f_2) + \mu P(\phi) \\ &= \lambda_1 \int \left[\int K_\sigma(x-y)|I(y)-f_1(x)|^2 H_\varepsilon(\phi)dy \right] dx + \\ &\lambda_2 \int \left[\int K_\sigma(x-y)|I(y)-f_2(x)|^2 (1-H_\varepsilon(\phi))dy \right] dx + \upsilon \int |\nabla H_\varepsilon(\phi)|\, dx \\ &+ \frac{1}{2}\mu \int (|\nabla\phi| - 1)^2 dx \end{aligned} \quad (12)$$

where $E_\varepsilon(\phi, f_1, f_2)$ is the external energy that depends upon the data of interest, μ>0 stands for the weights of regularization on the LSF ϕ , and $P(\phi)$ is the level set regularization term.

Step 3: Modify the fitting functions of $f_1(x)$ and $f_2(x)$.

Steepest descent method is used to minimize the energy functional in Equation (12) with respect to the functions of $f_1(x)$ and $f_2(x)$. In calculus of variations, it is shown that the function $f_1(x)$ and $f_2(x)$ minimizing Equation (12), satisfy the Euler-Lagrange equation as

$$\int K_\sigma(x-y)|I(y)-f_1(x)|^2 H_\varepsilon(\phi)dy+\int K_\sigma(x-y)|I(y)-f_2(x)|^2(1-H_\varepsilon(\phi))dy=0 \quad (13)$$

The function of $f_1(x)$ is shown below.

$$f_1(x)=\frac{\int K_\sigma(x-y)I(y)H_\varepsilon(\phi)dy}{\int K_\sigma(x-y)H_\varepsilon(\phi)dy} \quad (14)$$

Equation (14) can be rewritten as the convolution-like form

$$f_1(x)=\frac{K_\sigma(x)*[H_\varepsilon(\phi)f(x,y)]}{K_\sigma(x)*H_\varepsilon(\phi)} \quad (15)$$

where

$K_\sigma(x)$: Kernel in point *x*

$f(x,y)$: Enhanced pixel value of 2D sigmoid function

$H_\varepsilon(\phi)$: smoothed Heaviside function

This form indicates that $f_1(x)$ is a weighted average of the intensities in a neighbourhood of *x*.

The function of $f_2(x)$ is shown below.

$$f_2(x)=\frac{\int K_\sigma(x-y)I(y)(1-H_\varepsilon(\phi))dy}{\int K_\sigma(x-y)(1-H_\varepsilon(\phi))dy} \quad (16)$$

Similar to the Equation (15), Equation (16) can be rewritten as the convolution-like form,

$$f_2(x)=\frac{K_\sigma(x)*[(1-H_\varepsilon(\phi))f(x,y)]}{K_\sigma(x)*(1-H_\varepsilon(\phi))}=\frac{K_\sigma(x)*[f(x,y)-H_\varepsilon(\phi)f(x,y)]}{(K_\sigma(x)*1)-(K_\sigma(x)*H_\varepsilon(\phi))} \quad (17)$$

This form indicates that $f_2(x)$ is a weighted average of the intensities in a neighbourhood of *x*.

Convolution term has been seen in the numerators and denominators of Equation (15) and Equation (17). The convolution is used by allowing two arrays of numbers to be multiplied together. The arrays can be different sizes but must be of the same dimension. In image analysis this process is generally used to produce an output image where the pixel values are linear combinations of certain input values. The terms of $K_\sigma(x)*1$ and $K_\sigma(x)*f(x,y)$ in Equation (17) do not depend on the evolving of the LSF, ϕ. Both can be computed only once before the number of iteration.

Step 4: Minimize energy function

Setting the $f_1(x)$ and $f_2(x)$ fixed, then minimize the Equation (12) with respect to ϕ using the gradient descent method by solving gradient flow equation as follows

$$\frac{\partial\phi}{\partial t}=-\delta_\varepsilon(\phi)(\lambda_1 e_1-\lambda_2 e_2)+\upsilon\delta_\varepsilon(\phi)div\left(\frac{\nabla\phi}{|\nabla\phi|}\right)+\mu\left(\nabla^2\phi-div\left(\frac{\nabla\phi}{|\nabla\phi|}\right)\right) \quad (18)$$

where

$$e_i(x)=\int K_\sigma(y-x)|I(x)-f_i(y)|^2 dy, \text{ for } \quad i=1,2 \quad (19)$$

The first term in Equation (18) is derived from the data fitting energy, and known as data fitting term. The main computational cost in this method computes Equation (15), Equation (17) and $(\lambda_1 e_1-\lambda_2 e_2)$ in the level set evolution. Therefore, MRF method applies into Equation (15) and Equation (17) to reduce the computational cost. The fitting values of $f_1(x)$ and $f_2(x)$ according to Equation (15) and Equation (17) should be computed to obtain Equation (19).

The second term of Equation (18) smoothing the zero level contours which maintain the regularity of the contour. This term is called the arc length term. The third term in Equation (18) is called the level set regularization term, since it serves to maintain the regularity of the level set function.

Step 5: Segment the tumour

The modification of region fitting energy is done in the data fitting term, $(\lambda_1 e_1-\lambda_2 e_2)$. The enhanced image of 2D sigmoid function supports the proposed model for driving the active contour toward tumour boundaries.

The size of pixel used in the original brain MRI image is 200 x 200 in jpeg format. There are parameters $\lambda, \mu, \sigma, \alpha, \beta, \nu$ and the time step Δt for the implementation. The method is not

sensitive to the choice of μ, which can be fixed for most of applications. These parameters are fixed as μ=1, ε =1.0, time step = 0.1 in this research. In this experiment, the setting values of λ_1 and λ_2 is equal to 1.0 which the weights of the two integrals.

The parameters $\alpha, \beta, \nu, \sigma$ needs to be tuned for different images. The experimental study choose C_0=2 as the initial LSF, ϕ_0 for the MRF method which new contour can emerge easily and the curve evolution is significantly faster than the evolution from an initial function as a signed distance map. The implementation of the experiments used Matlab at Windows.

IV. Result and Discussion

This section shows the result of implementation of segmentation method for detecting tumour region. The red mark shows the boundaries of tumour contour. The method has been tested for 5 enhanced tumour images and the MRF method performs on different initial contour for 5 MRI brain images, Figure 2-11. To implement the segmentation of tumour, the scale parameter of Gaussian kernel is $\sigma = 3.0$. The parameter denotes the radius of the neighbourhood closed related to the degree of the intensity inhomogeneity. A smaller value of σ is more suitable for tumour region with more localized intensity inhomogeneity. Parameter $\sigma = 3.0$ has $\omega = 13$ and the size of mask is 13 by 13. The mask is used to detect the edges of the tumour image.

The parameter υ in the second term of the Equation (16) smoothed the zero level contour of tumour. For example, the value of scale parameter in image of Tumour 1 is $\sigma = 3.0$ and the value of υ are 0.2 x 255 x 255.

Figure 2 shows the initial contour of tumour at ϕ=0 for t = 0. The initial LSF, ϕ_0 is C_0=2 at (55:105, 70:110). The binary step function is used for speed up the contour evolution [9]. The emergence of new contours speeds up the curve evolution toward final results, and enables the detection of interior boundaries in Figure 2.

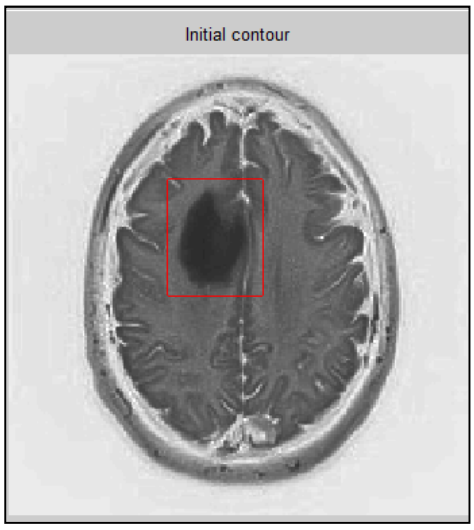

Fig. 2. The initial contours of Tumour 1.

The emergence of new contours is possible because the data fitting term in Equation (16) has influenced on the change of the entire image domain, as the factor $\delta_\varepsilon(\phi)$ is nonzero by definition in Equation (9).

As a result, the factor $\delta_\varepsilon(\phi)$ takes relatively larger values in the beginning of the level set evolution, which leads to faster emergence of new contours at strong edges, even at locations far away from current zero level set. In this experiment, the parameter value for ε is equal to 1.0 which gives the faster and accurate result of final region in Figure 3 after 350 iterations.

The enhanced image of tumour 1 marked with the segmentation result are shown in Figure 3. The segmentation result illustrates the clear region of tumour which MRF performs the final contour in 350 iterations.

Figure 4 represents the initial contour of tumour 2 ϕ=0 for t = 0. The initial LSF, ϕ_0 is C_0=2 (48:95, 100:138). The initial tumour in MR brain image has been shown in solid red contour with the parameter value, υ = 0.2 x 255 x 255.

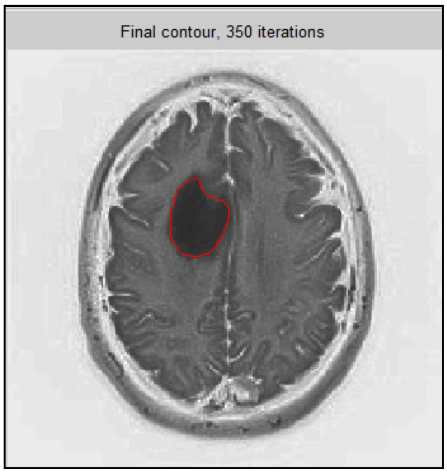

Fig. 3. The final contour of tumour 1 after 350 iterations.

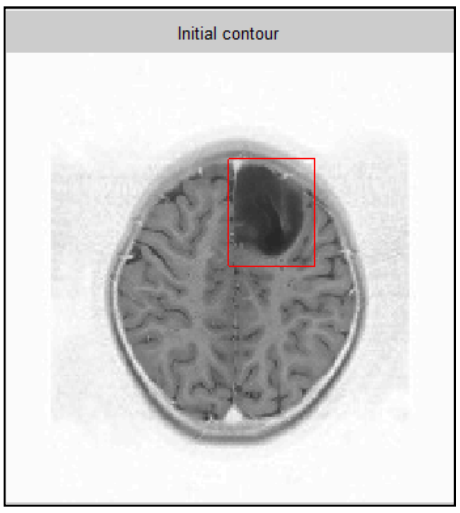

Fig. 4. The initial contour of Tumour 2.

The enhanced image of tumour 2 marked with the segmentation result are shown in Figure 5. The segmentation result illustrates the clear region of tumour which MRF performs the final contour in 250 iterations. The initial contour of tumour 3 at ϕ=0 for t = 0 is represented in Figure 6. The initial LSF ϕ_0 is C_0=2 at (63:116,120:154). The initial tumour in MR brain image has been shown in solid red contour with the parameter value, υ = 0.25 x 255 x 255.

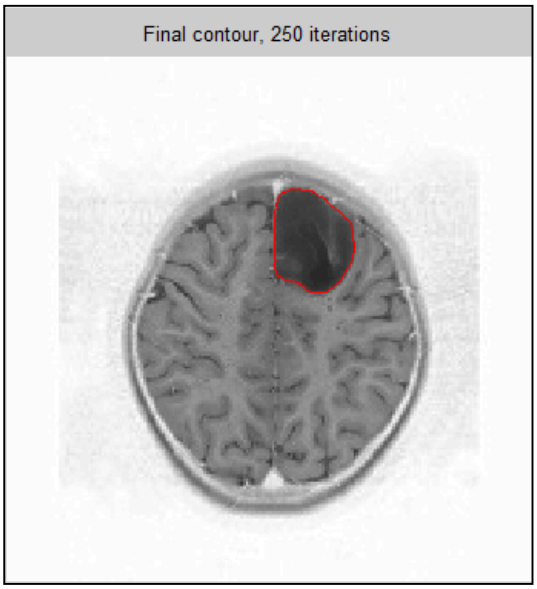

Fig. 5. The final contour of tumour 2 after 250 iterations.

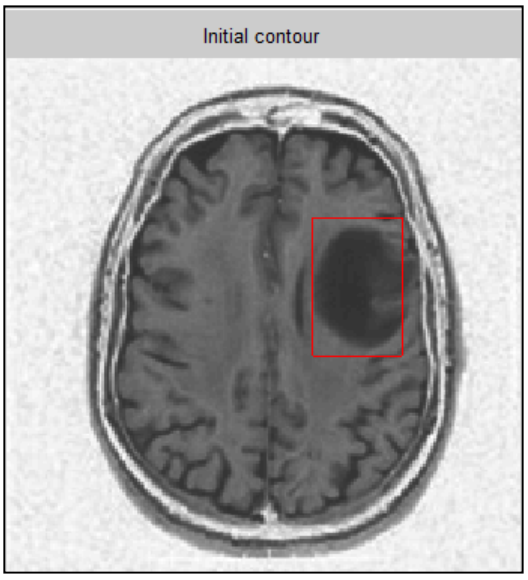

Fig. 6. The initial contour of Tumour 3.

The enhanced image of tumour 3 marked with the segmentation result are shown in Figure 7. The segmentation result illustrates the clear region of tumour which MRF performs the final contour in 490 iterations. Figure 8 represents the initial contour of tumour 4 at ϕ=0 for t = 0. The initial ϕ_0 is C_0=2 at (50:85, 60:90). The initial tumour in has been shown in solid red contour with the parameter value, υ = 0.45 x 255 x 255.

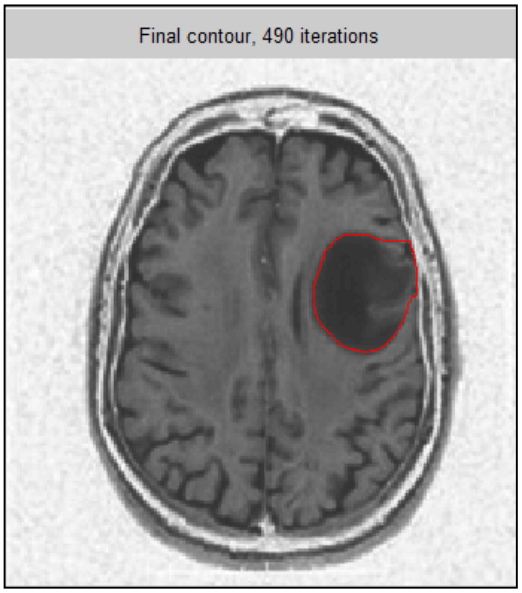

Fig. 7. The final contour of tumour 3 after 490 iterations.

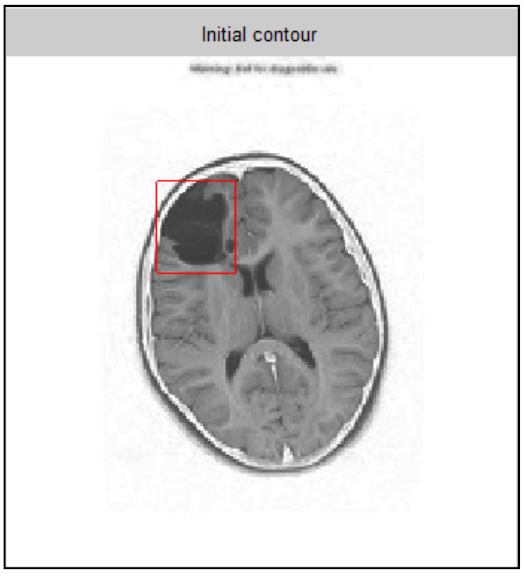

Fig. 8. The initial contour of Tumour 4.

The enhanced image of tumour 4 marked with the segmentation result are shown in Figure 9. The segmentation result illustrates the clear region of tumour which MRF performs the final contour in 600 iterations. The initial contour of tumour 5 is shown in Figure 10 at ϕ=0 for t = 0. The initial LSF ϕ_0 is C_0=2 at (100:168, 107:148). The initial tumour in MR brain image has been shown in solid red contour with the parameter value, υ = 0.2 x 255 x 255.

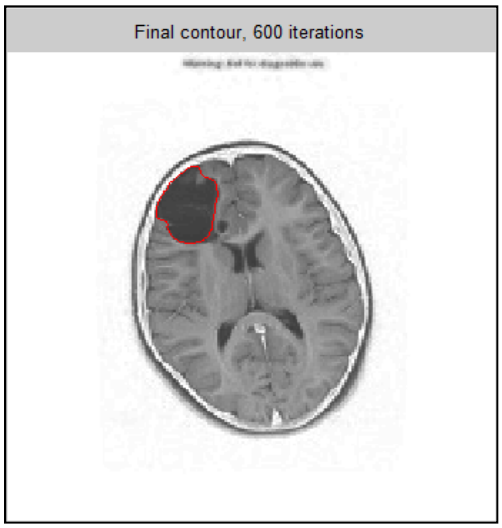

Fig. 9. The final contour of tumour 4 after 600 iterations

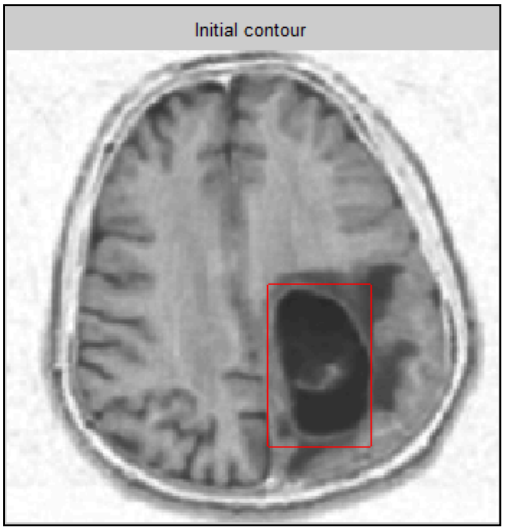

Fig. 10. The initial contour of Tumour 5.

The enhanced image of tumour 5 marked with the segmentation result are shown in Figure 11. The segmentation result illustrates the clear region of tumour which MRF performs the final contour in 250 iterations. From the segmentation results of initial region of tumour 1 to 5, the number of iterations can be summarized in the following Table I.

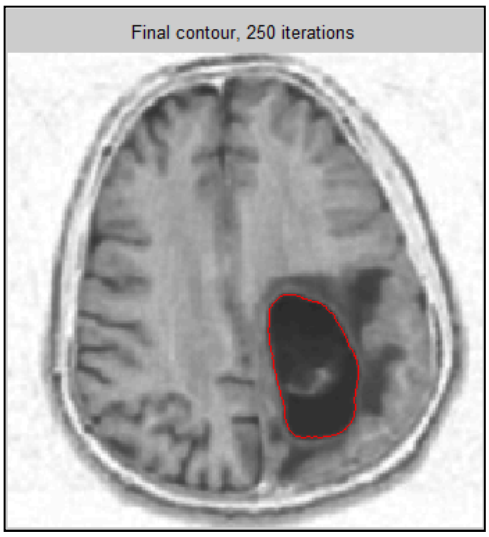

Fig. 11. The final contour of tumour 5 after 250 iterations.

TABLE I. THE NUMBER OF ITERATIONS FOR MRF METHOD OF TUMOUR 1 TO 5.

	Tumour 1 **200 x 200 pixel**	**Tumour 2** **200 x 200 pixel**	**Tumour 3** **200 x 200 pixel**	**Tumour 4** **200 x 200 pixel**	**Tumour 5** **200 x 200 pixel**
MRF	380	340	450	700	300

Based on Figures 2-11 and the number of iteration in Table I, the MRF method has been successfully to segment the initial region of brain tumour images.

V. CONCLUSION

The experiments have been done for 5 MRI brain images which contain brain tumour. Clearly, the experiments have shown that the MRF method has successfully segmented the initial region of brain tumour images. For the future works, the performance of Modified Region Scalable Fitting (MRSF) would be evaluated by comparing the number of iterations with the Region Scalable Fitting (RSF) method and Experimental in terms of computation efficiency. Success in the brain image segmentation will ultimately help the doctors for tumour detection and they may group the tumour by grade.

ACKNOWLEDGMENT

This research is a continuation of a published paper with DOI:10.1109/eecsi.2017.8239103 and partially used a funding from Fundamental Research Grant Scheme (FRGS/1/2016/STG07/) – Pure and Applied Science.

REFERENCES

[1] S. Widyarto, S. R. B. Kassim, and W. K. Sari, "2D-sigmoid enhancement prior to segment MRI glioma tumour: Pre image-processing," in *International Conference on Electrical Engineering, Computer Science and Informatics (EECSI)*, 2017, vol. 2017-Decem.

[2] S. Mas *et al.*, "Use of physiological information based on grayscale images to improve mass spectrometry imaging data analysis from biological tissues," *Anal. Chim. Acta*, 2019.

[3] K. M. Meiburger *et al.*, "Automatic Skin Lesion Area Determination of Basal Cell Carcinoma using OCT Angiography and a Skeletonization Approach: Preliminary Results," *J. Biophotonics*, p. e201900131, 2019.

[4] Z. N. Khan Swati *et al.*, "Brain tumor classification for MR images using transfer learning and fine-tuning," *Comput. Med. Imaging Graph.*, 2019.

[5] P. Korfiatis and B. Erickson, "Deep learning can see the unseeable: predicting molecular markers from MRI of brain gliomas," *Clin. Radiol.*, vol. 74, no. 5, pp. 367–373, 2019.

[6] E. Nagarathinam and T. Ponnuchamy, "Image registration-based brain tumor detection and segmentation using ANFIS classification approach," *Int. J. Imaging Syst. Technol.*, no. November 2018, p. ima.22329, 2019.

[7] C. Li, C. Y. Kao, J. C. Gore, and Z. Ding, "Minimization of region-scalable fitting energy for image segmentation," *IEEE Trans. Image Process.*, vol. 17, no. 10, pp. 1940–1949, 2008.

[8] S. Osher and J. A. Sethian, "Fronts propagating with curvature-dependent speed: Algorithms based on Hamilton-Jacobi formulations," *J. Comput. Phys.*, vol. 79, no. 1, pp. 12–49, 1988.

[9] T. Liu, H. Xu, W. Jin, Z. Liu, Y. Zhao, and W. Tian, "Medical Image Segmentation Based on a Hybrid Region-Based Active Contour Model," *Comput. Math. Methods Med.*, vol. 2014, pp. 1–10, 2014.